catalysts

MDPI

Article

Synthesis, Stereochemical and Photophysical Properties of Functionalized Thiahelicenes

Valentina Pelliccioli [1,2], Francesca Cardano [1], Giacomo Renno [3], Francesca Vasile [1], Claudia Graiff [4], Giuseppe Mazzeo [5], Andrea Fin [6], Giovanna Longhi [5,7], Sergio Abbate [5,7], Alessia Rosetti [8], Claudio Villani [8], Guido Viscardi [3], Emanuela Licandro [1] and Silvia Cauteruccio [1,*]

1 Dipartimento di Chimica, Università degli Studi di Milano, Via Golgi 19, 20133 Milan, Italy; valentina.pelliccioli@unimi.it (V.P.); francesca.cardano@unimi.it (F.C.); francesca.vasile@unimi.it (F.V.); emanuela.licandro@unimi.it (E.L.)
2 Institut für Organische und Biomolekulare Chemie, Georg-August-Universität Göttingen, Tammannstr. 2, 37073 Göttingen, Germany
3 Dipartimento di Chimica, Università degli Studi di Torino, Via P. Giuria 7, 10125 Torino, Italy; giacomo.renno@unito.it (G.R.); guido.viscardi@unito.it (G.V.)
4 Dipartimento di Scienze Chimiche, della Vita e della Sostenibilità Ambientale, Università di Parma, Parco Area delle Scienze 17/a, 43124 Parma, Italy; claudia.graiff@unipr.it
5 Dipartimento di Medicina Molecolare e Traslazionale, Università di Brescia, Viale Europa 11, 25123 Brescia, Italy; giuseppe.mazzeo@unibs.it (G.M.); giovanna.longhi@unibs.it (G.L.); sergio.abbate@unibs.it (S.A.)
6 Department of Drug Science and Technology, University of Turin, Via P. Giuria 9, 10125 Torino, Italy; andrea.fin@unito.it
7 Istituto Nazionale di Ottica (INO), CNR, Research Unit of Brescia, c/o CSMT, VIA Branze 45, 25123 Brescia, Italy
8 Dipartimento di Chimica e Tecnologie del Farmaco, Sapienza Università di Roma, P.le A. Moro 5, 00185 Roma, Italy; alessia.rosetti@uniroma1.it (A.R.); claudio.villani@uniroma1.it (C.V.)
* Correspondence: silvia.cauteruccio@unimi.it; Tel.: +39-02-50314147

Abstract: We report on the synthesis of a novel class of functionalized thia[6]helicenes and a thia[5]helicene, containing a benzothiophene unit and a second heteroatom embedded in the helix (i.e., nitrogen and oxygen) or a pyrene or a spirobifluorene moiety. These systems are obtained through straightforward and general procedures that involve: (i) palladium-catalyzed annulation of iodo-atropoisomers with internal alkynes and (ii) Suzuki coupling of iodo-atropoisomers with phenyl boronic acid followed by a Mallory-type reaction. Both experimental and theoretical studies on the configurational stability of some selected thia[6]helicenes confirmed their stability toward racemization at room temperature, while the pyrene-based thia[5]helicene was found to be unstable. Moreover, the configuration assignment for one representative thiahelicene was established through the comparison between experimental and theoretical circular dichroism (CD) spectra. A systematic study of the photophysical properties of both thiahelicenes and the corresponding atropoisomers has been carried out to provide a complete overview on the new molecules proposed in this work. The obtained data showed regular trends in all the thiahelicene series with spectroscopic traits in line with those previously observed for similar heterohelicenes.

Keywords: thiahelicenes; synthetic methodology; palladium catalysts; annulation reactions; HPLC; circular dichroism; DFT calculations

Citation: Pelliccioli, V.; Cardano, F.; Renno, G.; Vasile, F.; Graiff, C.; Mazzeo, G.; Fin, A.; Longhi, G.; Abbate, S.; Rosetti, A.; et al. Synthesis, Stereochemical and Photophysical Properties of Functionalized Thiahelicenes. *Catalysts* **2022**, *12*, 366. https://doi.org/10.3390/catal12040366

Academic Editor: Gianluigi Albano

Received: 3 March 2022
Accepted: 22 March 2022
Published: 23 March 2022

1. Introduction

Nowadays, helicenes are among the most investigated classes of nonplanar chiral polycyclic aromatic compounds, thanks to their inherent helical chirality in combination with the extended π-conjugated structure [1–3]. Helicenes are made of *ortho*-fused benzene or other (hetero)aromatic rings, which adopt a nonplanar screw-shaped skeleton due to the steric repulsive interaction between the terminal rings (Chart 1). The highly delocalized

helical π–electron system confers them with enhanced chiroptical properties including circular dichroism (CD) [4] and circularly polarized luminescence (CPL) [5]. Therefore, they have been proposed in a plethora of cutting-edge applications including nonlinear optics, chiral sensors, and asymmetric catalysis, to name a few [2,3]. The introduction of heteroatom(s) in the helical skeleton significantly affects the geometric parameters and the electronic structure of the helix, providing unique functions and chiroptical response: this clearly strengthens the interest toward the heterohelicenes and helicenoid subgroups [6–8]. Additionally, the modification of the helicene core derived from a lateral extension of the π-conjugated systems [9,10], occurring, for example, in pyrene–helicene hybrids [11–23], affords compounds with enhanced functional properties.

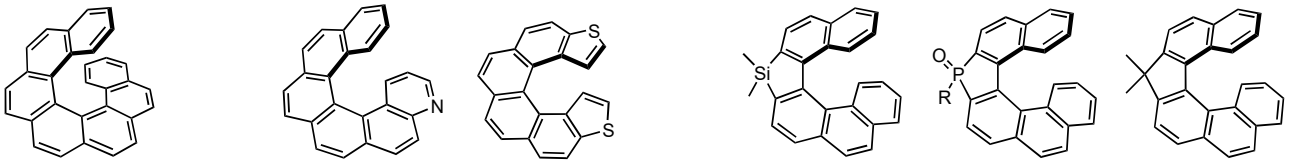

carbohelicene heterohelicenes helicene-like compounds

Chart 1. General structure of carbo, heterohelicenes, and helicene-like compounds.

Numerous synthetic approaches for the preparation of heterohelicenes have been so far reported [2,3,6,24–26], and they have played a key role in the progress of the helicene chemistry. However, they often provide a specific heterohelicene class, and lack versatility for the helicenes' structural diversity. Therefore, the search for some general and versatile methods to afford heterohelicenes with structural diversity including kinds and positions of heteroatoms and numbers of constituent rings is still highly sought after.

From this perspective, thiahelicenes, containing *ortho*-fused thiophene and benzene rings, represent versatile structures since the dibenzothiophene moiety in the helical framework can be easily modified through the so-called "aromatic metamorphosis" [27–31] to provide a wide range of different heterohelicenes [32,33]. On the other hand, thiahelicenes have received considerable attention due to the combination of both chiroptical properties of the helix along with electronic properties inferred by the presence of sulfur atoms [34,35]. Over the years, we have been interested in the synthesis and functionalization of tetrathia[7]helicenes (7-TH), which are a class of configurationally stable thiahelicenes, and are appealing candidates in non-linear optics [36–42], self-assembly [43–45], enantioselective electroanalysis [46], catalysis [47–50], and biology [51–55]. Our recent efforts have indeed been focused on finding diversity-oriented synthetic methodologies to synthesize the 7-TH scaffold through transition metal catalyzed annulation reactions of atropoisomeric bis(benzodithiophene) derivatives [56]. In particular, 2-bromo-3,3′-bibenzo[1,2-*b*:4,3-*b*′]dithiophenes **I** have been highlighted as useful intermediates to smoothly obtain 7,8-disubstituted 7-TH **II** through the Pd-catalyzed annulation of internal alkynes (Figure 1a). Benzo fused 7-TH **III** could instead be efficiently prepared by a two-step procedure involving the Suzuki coupling of bromides **I** with boronic acids followed by a Mallory-type reaction of intermediates **IV** (Figure 1a).

The efficacy and flexibility of this recent study prompted us to extend the aforementioned strategies for the synthesis of thiahelicenes with structural diversity including kinds of endocyclic heteroatoms and numbers of constituent rings, starting from the benzothiophene-based iodides **V** (Figure 1b).

Herein, we describe the synthesis and characterization of novel thia[6]helicenes **1a–c** and the corresponding benzo fused derivatives **2a–c**, containing carbazole, dibenzofuran, dibenzothiophene units (Figure 1c). Furthermore, the first example of a pyrene-heterohelicene hybrid such as pyrene-thiahelicene **3** has been synthesized, along with the spirobifluorene-thiahelicene hybrid **4** (Figure 1c). The stereochemical properties and the absolute configuration were established through circular dichroism (CD) spectra on enantiomerically separated samples previously resolved by high performance liquid

chromatography (HPLC) methods and by comparison with density functional theory (DFT) calculations.

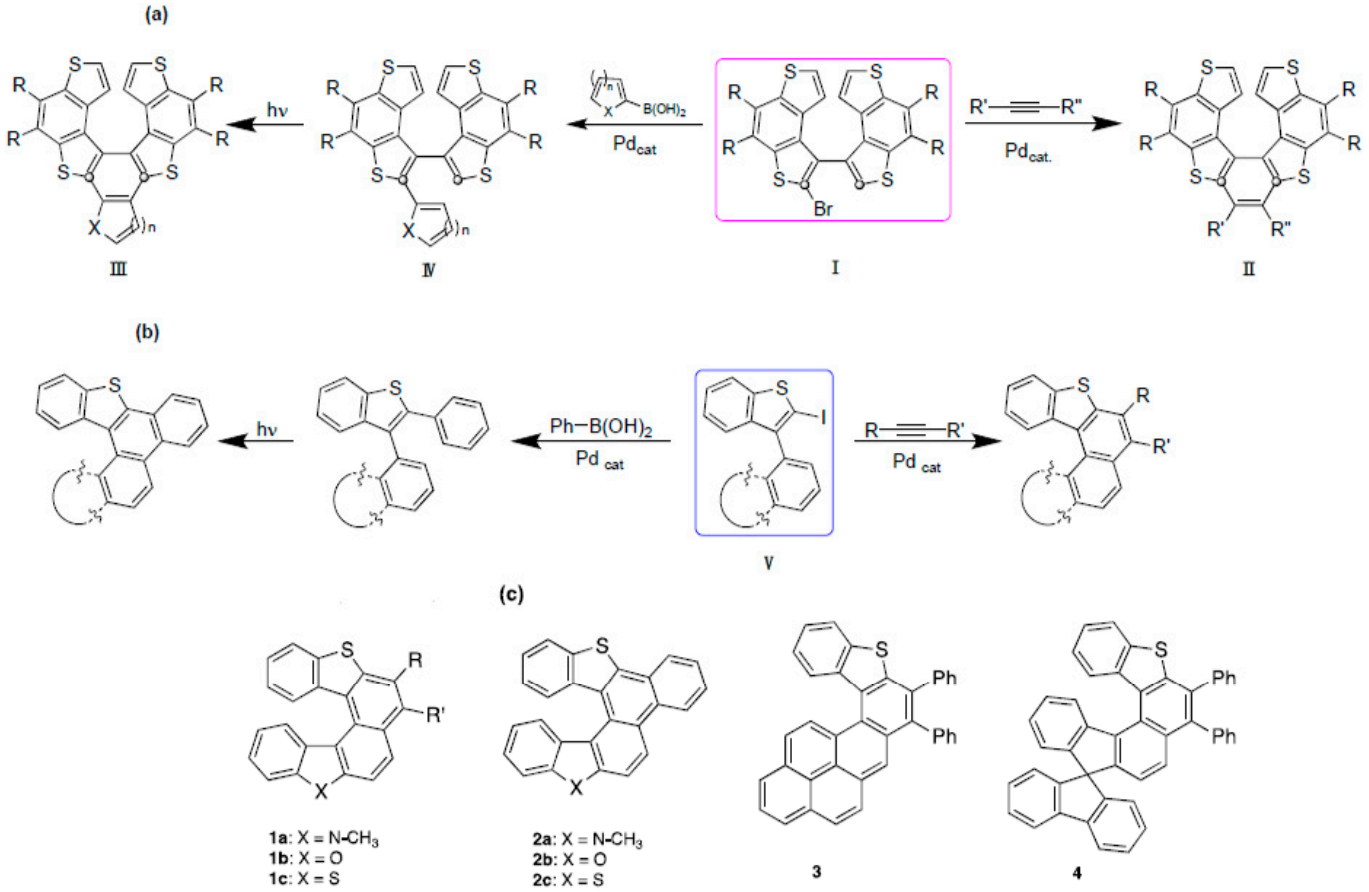

Figure 1. Synthetic strategies for the synthesis of 7-TH and novel thiahelicenes. (**a**) Previous work, (**b**) this work and (**c**) thiahelicenes developed in this work.

Finally, the photophysical properties of the new compounds obtained in this work including the thiahelicenes and the atropoisomeric intermediates were fully investigated by means of UV–Vis absorption and fluorescence emission measurements at room temperature in a diluted solution to shed light on these new families of thiahelicenes.

2. Results

2.1. Synthesis, NMR Studies, and X-ray Characterization

2.1.1. Synthesis of Bi(hetero)aryls **5a–c**, **6**, and **7**

The first step for the synthesis of thiahelicenes **1**–**4** involves the preparation of bi(hetero)aryls **5a–c**, **6**, and **7** as key intermediates to have access to iodides **V** (Figure 1b). Compounds **5a–c**, **6**, and **7** were prepared through the Suzuki reaction between the commercially available benzothienyl boronic acid (**8**) and the easily available polycyclic heteroaromatic bromides including 4-bromo-9-methyl-9*H*-carbazole (**9a**) [57], 1-bromodibenzofuran (**9b**), 1-bromodibenzothiophene (**9c**), 1-bromopyrene (**10**), and 4-bromo-9,9′-spirobi[9*H*-fluorene] (**11**). In particular, these reactions were performed in the presence of 1.4 equiv. of boronic acid **8**, 10 mol% of tetrakis(triphenylphosphine) palladium(0) as catalyst, and 1.4 equiv. of Cs_2CO_3 as base in dry DMF at 80 °C (Scheme 1), according to similar reaction conditions reported for the Suzuki coupling of boronic acid **8** with aryl bromides [58].

After 8–11 h, no presence of starting bromide was observed in the reaction mixture and the desired bi(hetero)aryls **5a–c**, **6**, and **7** were isolated, providing the required products in excellent yields (92–98%). The reduction in the catalyst amount from 10 to 5 mol% was tested with no success, providing indeed a lower yield (see Scheme S1, SM).

The NMR assignment for **5a–c**, **6**, **7** and for all new compounds obtained in this work was carried out using different experiments, requiring a detailed and sophisticated spectroscopic investigation. In particular, the complete ^{1}H and ^{13}C NMR assignments (Tables S1–S27, SM) were determined based on 1D and 2D NMR spectra (^{1}H and ^{13}C NMR, Correlation SpectroscopY COSY, Heteronuclear Single Quantum Coherence HSQC, and Heteronuclear Multiple Bond Correlation HMBC). 2D-COSY experiments were used for the identification of neighboring protons, and to solve ambiguity in the assignment, 2D-NOESY (Nuclear Overhauser Effect SpectroscopY) experiments were used to observe homonuclear correlation via dipolar coupling. ^{1}H-^{13}C HSQC experiments were performed to confirm and follow the resonances of carbons. The identification of quaternary carbons was performed analyzing ^{13}C APT (Attached Proton Test) and ^{1}H-^{13}C HMBC experiments. Using ^{1}H-^{13}C HMBC and following the long-range proton-carbon correlations (especially between atoms separated by three covalent bonds), it was possible to uniquely assign most of the quaternary carbons.

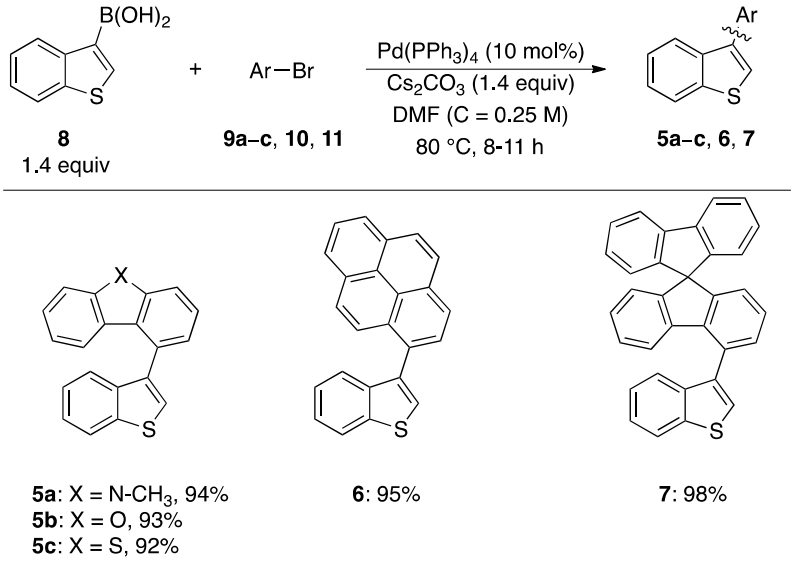

Scheme 1. Synthesis of bi(hetero)aryls **5a–c**, **6**, and **7**.

2.1.2. Synthesis of Iodides **12a–c**, **13**, and **14**

Biaryls **5a–c**, **6**, and **7** were found to be convenient starting materials to obtain the corresponding iodides **12a–c**, **13**, and **14**, which can be prepared through the deprotonation of the α-position of the benzothienyl moiety of **5a–c**, **6**, and **7** and the reaction with iodine (Scheme 2).

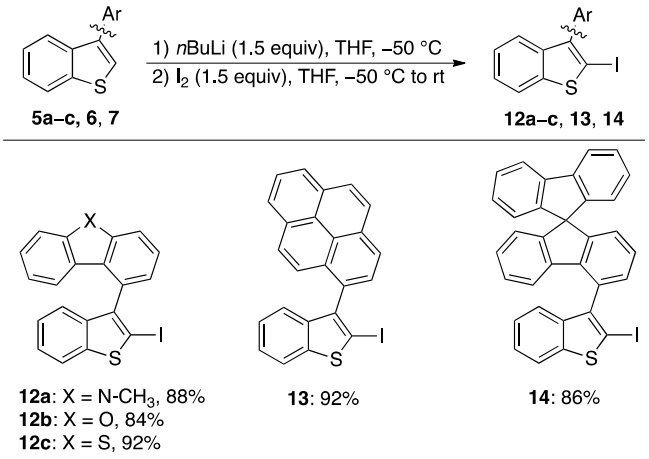

Scheme 2. Synthesis of iodides **12a–c**, **13**, and **14**.

In particular, iodides **12a–c** were isolated in high yields (84–92%) by the treatment of a solution of biaryl **5a–c** in dry THF (C = 0.75 M) with 1.5 equiv of *n*BuLi at −50 °C followed by the addition of a solution of iodine (1.5 equiv) in THF (Scheme 2). The iodination of biaryls **6** and **7** was performed under similar experimental conditions, but in this case, a more diluted solution of **6** and **7** in THF (C = 0.10 M) was used due to their lower solubility. However, these diluted conditions did not affect the reactions' efficacy, providing iodides **13** and **14** in 92 and 86% yields, respectively. Of note, the crude products of these reactions contained only the required iodides, and no starting materials or by-products were observed. The crudes were indeed washed with diethyl ether and pentane, and used in the following steps, without further purification. The regioselectivity of iodination was confirmed by NMR spectroscopy (see Tables S6–S10, SM), since the signals corresponding to the proton close to S (a singlet around 7.2–7.25 ppm) disappear. Moreover, the directly bonded carbon atom (with a chemical shift around 124–125 ppm in compounds **5a–c**, **6**, and **7**) becomes quaternary and the replacement of hydrogen by iodine results in the shielding typical of the heavy-atom α-effect (its chemical shift value is around 82 ppm).

2.1.3. Palladium-Catalyzed Annulation of Alkynes by Iodides **12a–c**, **13** and **14**

Having secured access to iodides **12a–c**, **13**, and **14**, we sought to take advantage of these intermediates for the synthesis of novel classes of thiahelicenes **1**, **3**, and **4** through the palladium-catalyzed carboannulation of internal alkynes **15** (Scheme 3). The palladium-promoted hetero and carboannulation reactions of alkenes, dienes, or alkynes have been extensively studied by Larock and co-workers to prepare a wide range of heterocycles and carbocycles [59,60]. Initially, we performed this reaction under experimental conditions very similar to those reported by Larock et al. for the synthesis of phenantrene-like structures [61]. Thus, iodides **12a–c**, **13**, and **14** were reacted with 1.5 equiv of internal alkynes **15a–c** in the presence of 5 mol% of $Pd(OAc)_2$, 2 equiv of NaOAc, and 1 equiv of LiCl in dry DMF at 100 °C for 9 h (Scheme 3).

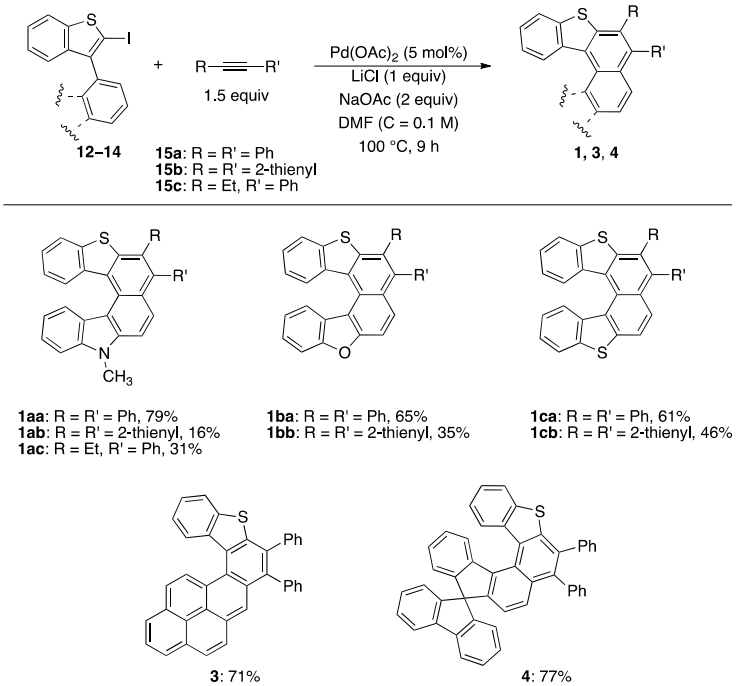

Scheme 3. Palladium-catalyzed annulation of alkynes **15** by iodides **12–14**.

The results reported in Scheme 3 demonstrate that the nature of the alkyne strongly affects the efficacy of these reactions, regardless of the nature of the iodide. Indeed, the carboannulation of diphenylacetylene (**15a**) afforded the corresponding thiahelicenes **1aa**, **1ba**, **1ca**, **3**, and **4** in good yields (61–79%), while the carboannulation of **15b** and **15c** resulted in being less effective, and the corresponding thia[6]helicenes **1ab**, **1bb**, **1cb**, and **1ac** were

isolated in lower yields (16–46%). It should be noted that no rearrangement that led to the formation of alkylidene fluorene-like derivatives was observed in these reactions. Furthermore, the annulation of unsymmetrical alkyne **15c** by iodide **12a** was found to be highly regioselective, yielding only the regioisomer **1ac** in 31% yield (Scheme 3). This regioselectivity is consistent with previous palladium-catalyzed acetylene annulation reactions [61–64], in which the thienyl group adds to the less hindered end of the alkyne (i.e., ethyl substituent) and the palladium moiety to the more hindered end (i.e., phenyl substituent).

The regiochemistry of **1ac** was suggested by NMR experiments (in the ^{1}H-^{13}C HMBC spectrum, a correlation peak between the CH_2 protons and the quaternary carbon in position 15 was present) and confirmed by X-ray analysis. The molecular structure of compound **1ac** is reported in Figure 2a.

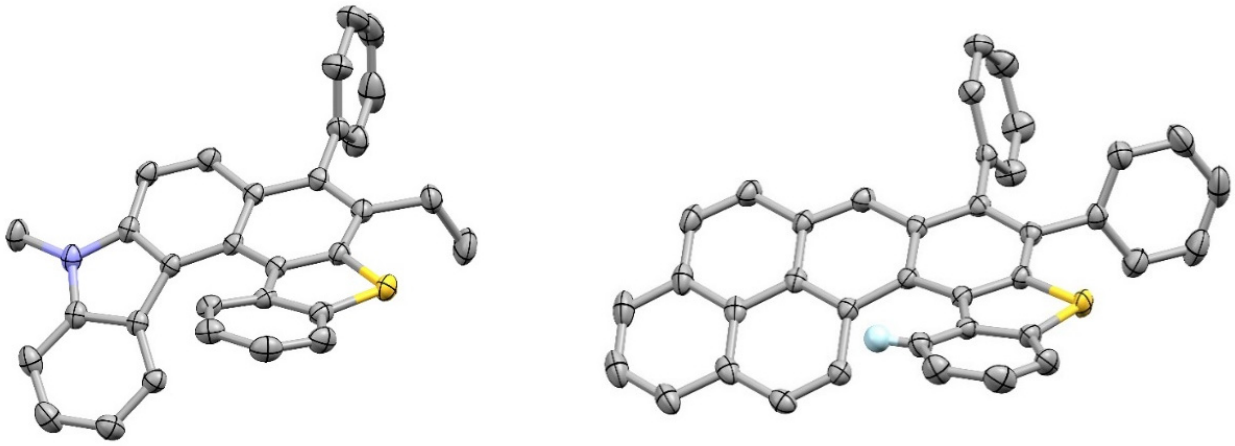

(**a**) (**b**)

Figure 2. ORTEP style view of enantiomer *M* for compounds **1ac** (**a**) and **3** (**b**). In compound **3**, hydrogen, represented in blue, corresponds to the doublet at 8.65 ppm in the ^{1}H NMR spectrum. Deposition number CCDC_2152004 (compound **1ac**); deposition number CCDC_2152005 (compound **3**).

The compound crystallizes in the chiral $P2_12_12_1$ space group and the molecule found was the enantiomer *M*. The naphthalene unit was slightly bent and the dihedral angle between the two benzene rings was 11.33(5)°. Considering all fused rings, the most tilted ones were those involving the two heteroatomic units with the naphthalene group being the dihedral angles 15.69(5) and 14.35(5)° for the pyrrole and thiophene rings, respectively. The dihedral angle between the two external benzene groups was 50.17(5)°. No strong π···π interactions were observed in the packing of the molecules, probably due to the position of the phenyl substituent, which was nearly orthogonal with respect to the mean plane of the naphthalene unit, preventing a close stacking of the molecules in the crystals. In agreement with what has been observed in the literature for other heterohelicenes [50,65–67], the C–C inner core bonds were longer than the typical 1.39 Å and the C–C outer core bond lengths were shorter. Single yellow crystals suitable for X-ray studies of pyrene-based thia[5]helicene **3** were also obtained. The crystals contained compound **3** together with cyclohexane solvent molecules. The ORTEP view of molecular structure of **3** is reported in Figure 2b. The compound crystallizes in the P-1 space group, so in the crystals, both enantiomers were present. The molecule adopted a helicene structure and can be depicted as a dibenzothiophene and a pyrene condensed group. The dihedral angle between the mean planes of the two components was 30.79(5)°. Additionally, in this case, the C–C inner core bonds were longer than the typical 1.39 Å. The two phenyl substituents were nearly orthogonal to the mean plane of the substituted benzene ring. However, two adjacent molecules could interact through π···π staking in the crystal packing at a distance of 3.70(5) Å.

The effect of the presence of pyrene moiety is strongly evident on the ^{1}H NMR spectra of **3**, especially on proton 9 of the dibenzothiophene ring (Table S18, SM). Its chemical shift (that in molecules with similar rings is between 7.4 and 8.0) corresponded to the doublet at 8.65 ppm due to the deshielding effect of the pyrene moiety. The crystal structure reported in Figure 2a clearly explains the values of the chemical shifts obtained for this molecule.

Concerning the NMR data for helicenes **1**, **3**, and **4**, ring-current effects can be particularly important, and the electron clouds of the aromatic rings can affect, through space, the resonances of aromatic protons on the other side of the molecule. They shift the resonances of the nuclei in the deshielding cone toward a higher chemical shift (in contrast, atoms below and above an aromatic system become more shielded, with a lower chemical shift) than similar nuclei in systems without this spatial interaction.

2.1.4. Synthesis of Benzo Fused Thiahelicenes **2a–c**

To further expand the usefulness of iodides **12–14**, we also considered the possibility of synthesizing benzo fused thiahelicenes **2** through a two-step procedure involving the Pd-catalyzed Suzuki coupling between **12–14** and phenyl boronic acid (**16**), followed by the Mallory-type cyclization. According to this synthetic route, intermediates **17a–c**, **18**, and **19** were synthesized by Suzuki reactions between **12–14** and two equivalents of **16** in the presence of $PdCl_2$(dppf) as the catalyst and KF as the base in a mixture of toluene and MeOH at 70 °C (Scheme 4).

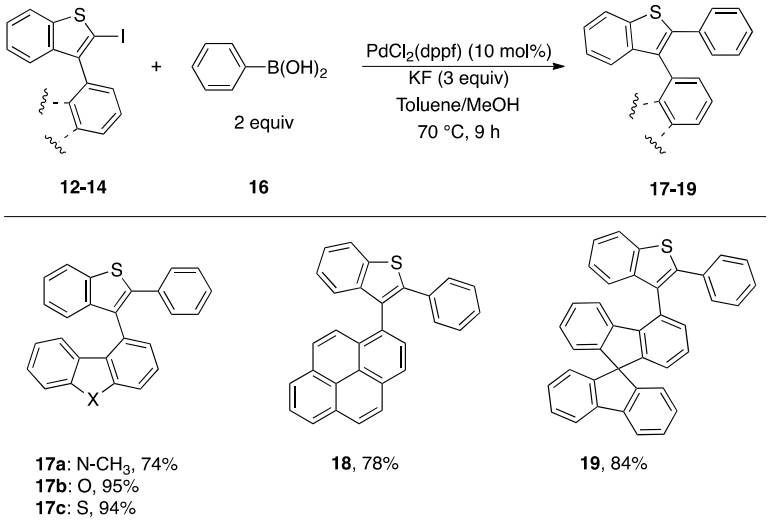

Scheme 4. Synthesis of intermediates **17–19**.

These experimental conditions, previously employed for the Suzuki coupling of aryl boronic acids with 2-bromo-3,3′-bibenzo[1,2-*b*:4,3-*b*′]dithiophenes (**I**) [56], were also found to be effective for the preparation of **17–19**, which were isolated in good yields (74–95%). Next, we preliminarily investigated the photocyclization of derivatives **17a–c**, **18**, and **19** under the experimental conditions similar to those used for the synthesis of benzo fused tetrathia[7]helicenes [56]. Thus, when a diluted solution of **17a–c** in cyclohexane was irradiated with a medium-pressure Hg lamp in the presence of a catalytic amount of iodine (10 mol%) at room temperature under air, the required thiahelicenes **2a–c** were isolated in moderate yields (Scheme 5).

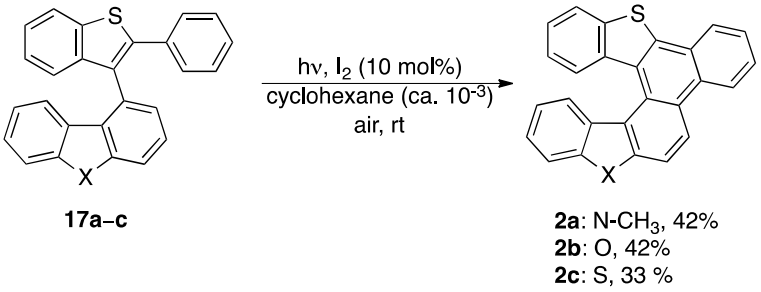

Scheme 5. Photocyclization of intermediates **17**–**19**.

Conversely, the photocyclization of **18** and **19** did not provide any cyclized products under the same conditions, and the starting materials were quantitatively recovered. This behavior could be ascribed to the lower electron-rich nature of the pyrene and spirobifluorene moieties in comparison with the carbazole, dibenzofuran, and dibenzothiophene portions. Indeed, oxidative photocyclization reactions are generally favored on electron-rich substrates. Another possible explanation could be related to the higher steric strain imparted by the pyrene moiety and steric congestion in spirobifluorene that hinder the formation of the twisted helical scaffold in the reported conditions. However, these preliminary experiments need further investigations (e.g., alternative photochemical conditions or Scholl-type reaction conditions), in order to promote these reactions.

2.2. Stereochemical Properties and Absolute Configuration

2.2.1. Configurational Stability

To evaluate the configurational stability of this novel class of thia[6]helicenes **1** and **2** and thia[5]helicene **3**, we selected a set of model derivatives including helicenes **1aa**, **1ba**, **1ca**, **2a**, **2b**, **2c**, and **3**. The enantiomers of helicenes **1aa**, **2a**, **2b**, and **2c** were easily separated by HPLC on the chiral stationary phase Chiralpak IA. Elution with hexane containing 20% of methylene chloride gave, in most cases, a chromatogram with two completely resolved peaks, with the same area and opposite response when monitored by circular dichroism detection (see Table S28, SM). The absence of enantiomeric separation for compounds **1ba** and **1ca** is certainly due to a lack of enantioselectivity of the chiral stationary phase and not to a fast enantiomerization, as the computed barriers to enantiomer interconversion are large enough to allow a physical separation at room temperature.

As expected, compound **3**, being a thia[5]helicene, is configurationally less stable, in analogy to what has been observed for other [5]helicenes [68,69], while, on the contrary, HPLC data indicate that [6]helicenes are stable at room temperature. We theoretically examined the racemization barriers by a comparison to [5]helicene **3**, with the cases **1aa**, **1ba**, and **1ca** presenting phenyl pendant groups and the analogous benzo fused helicenes **2a**, **2b**, and **2c**. Figure 3 presents the results obtained from relaxed scans (see SM for details).

Energy values of the transition states at M06-2X/cc-ptvz level were calculated, ensuring that they were true saddle points, and indeed they were: the calculated energy difference between the ground and transition state, corresponding to the racemization barrier, was 34 kcal/mol for the cases with two sulfur atoms, namely **1ca** and **2a**, 29 kcal/mol for **1aa** and **2a**, and 26 kcal/mol for **1ba** and **2b** with no substantial influence from the phenyl pendants compared to the benzo fused case and had close similarity to carbohelicene [1]. For compound **3**, the TS state was calculated at 18 kcal/mol above the ground state.

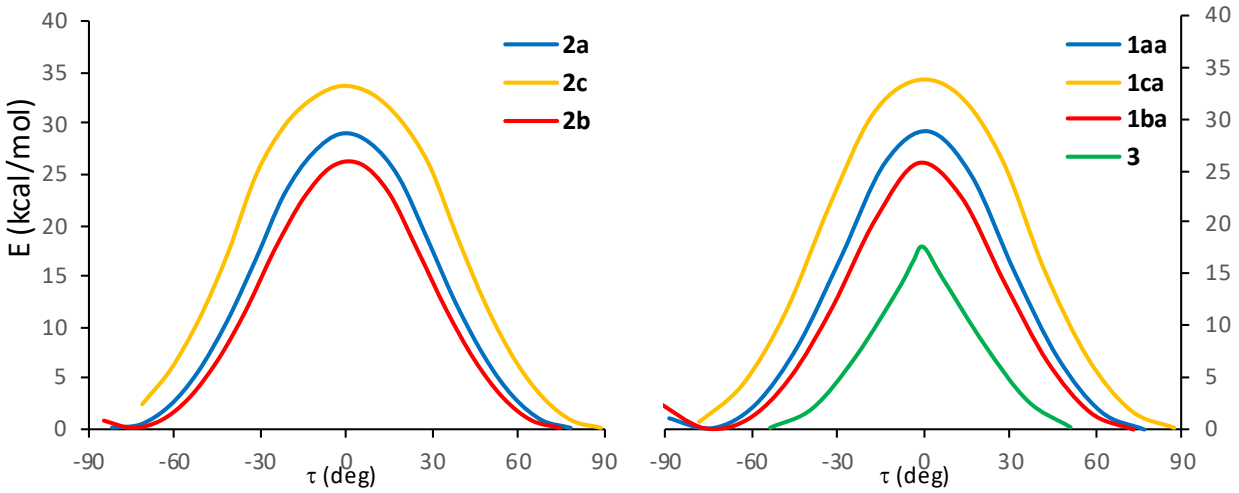

Figure 3. Relaxed scan along the racemization interconversion path obtained at M06-2X/6-31+g(d,p). Dihedral angle τ is defined in Figure S1. In the case of compounds presenting phenyl pendant groups, the curve is the minimal path of a double scan obtained by also relaxing the phenyl orientation with respect to the helicene backbone (see SM).

2.2.2. Assignment of Absolute Configuration of **2a**

To achieve a sufficient amount of single enantiomers for chiroptical characterization, 10 mg of racemic **2a** was dissolved in 2 mL of hexane/methylene chloride 80/20 and separated on a Chiralpak IA semipreparative column with a loading of 1 mg per run and a mobile phase composed by hexane containing 20% of methylene chloride. The first eluted enantiomer was collected with an optical purity of 96% while the second eluted was obtained with an enantiomeric excess of 86%.

After recording the CD spectra of the two fractions, to assign the absolute configuration, we optimized the structure for the *P* configuration and calculated the CD response via TD-DFT calculations. In Figure 4, a comparison is presented between the experimental and calculated spectra.

In the SM (Figure S2), a comparison with calculations at the M06 level is reported, obtaining a better match as far as wavelengths are concerned, while the shape of the spectrum was better reproduced by the theoretical spectrum presented in Figure 3 above: all features were present, even the two very weak ones observed at long wavelength. The two intense positive bands at 270 and 300 nm showed a larger separation in the calculated spectra; however, one can safely conclude that the first fraction corresponds to the *P*-configuration.

2.3. Photophysical Studies

The optical properties of all compounds, both intermediates and thiahelicenes, were evaluated in CH_2Cl_2 solutions (Table 1), and the data of the carbazole series are shown in Figure 5a as an example.

This set was accurately selected as the representative for the description because it contained the highest structural variability of the final thiahelicenes synthesized among all the series introduced in this work. The results presented (Figure 5b) highlights typical photophysical traits for helicene compounds with broadly intense absorption between 250 and 450 nm and emissions located in the 350–550 nm range. The photophysical parameters obtained were comparable with similar data already reported for other helicene structures bearing carbazole [70], pyrene [21], spirobifluorene [33], and dibenzothiophene [71] subunits in the helical scaffolds. These optical features are also in line with values observable for tetrathia[7]helicenes already investigated by our group [67], nevertheless showing in this last comparison a significant red-shift for pyrene and carbazole derivatives only.

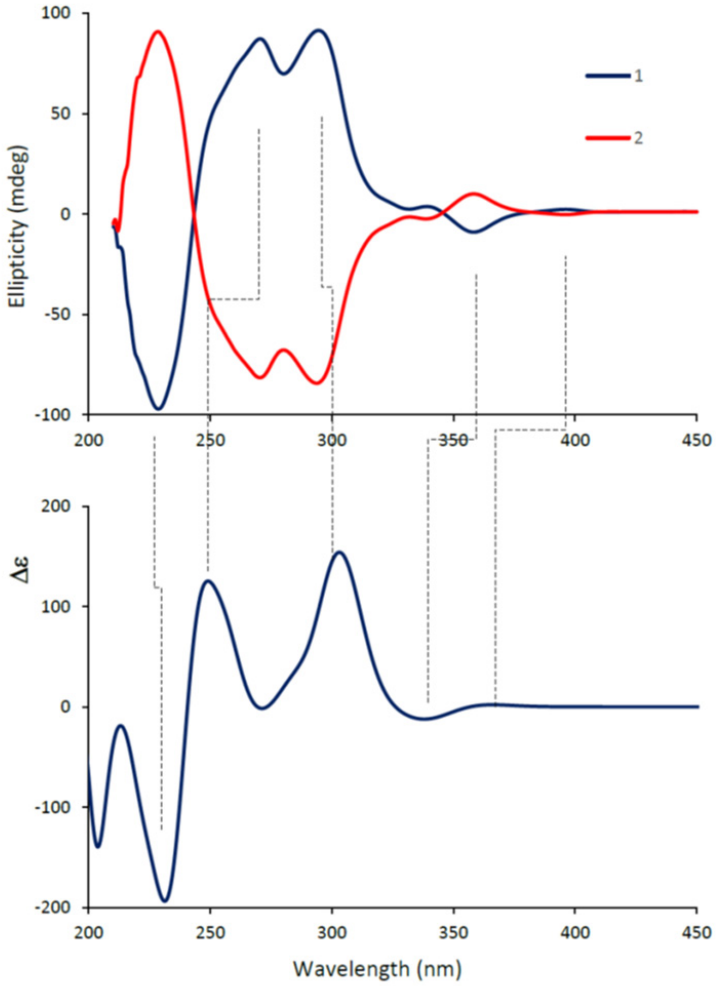

Figure 4. (**top**) Experimental CD spectra for the two enantiomers of **2a**. (**bottom**) Calculated CD spectrum for the P structure of **2a** at M06-2X/cc-pvtz level, bandwidth 0.2 eV, wavelength shift +25 nm.

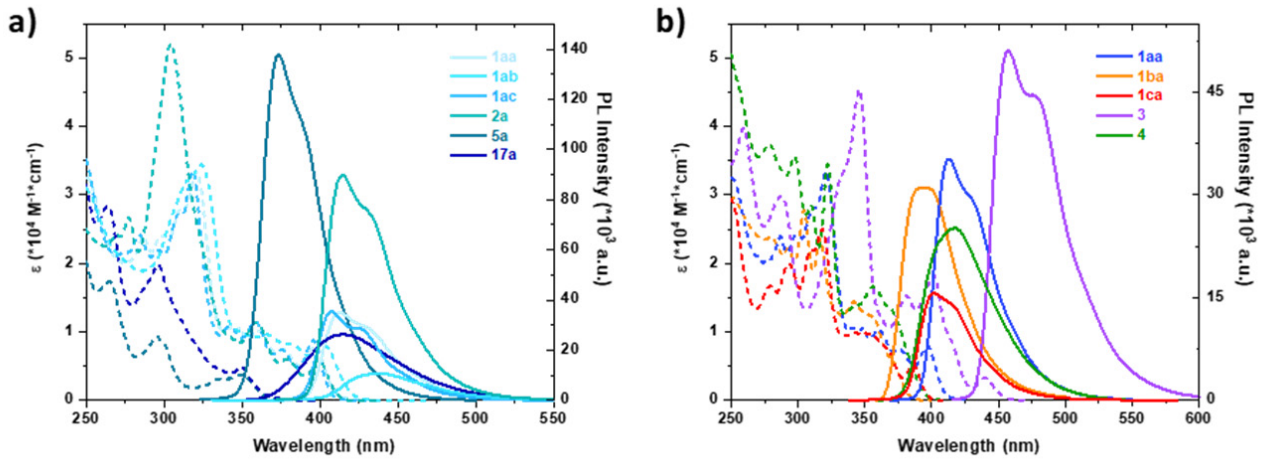

Figure 5. (**a**) Absorption (dashed) and emission (solid) spectra in CH_2Cl_2 of carbazole-based thiahelicenes and the intermediates **5a** and **17a**. (**b**) Absorption (dashed) and emission (solid) spectra in CH_2Cl_2 of the thiahelicenes bearing two pending phenyl groups and prepared within this work. Emission spectra were normalized to 0.1 intensity at excitation wavelength.

Table 1. Photophysical data of CH_2Cl_2 for thiahelicenes and relative intermediates.

Entry	λ_{abs} [1]	log ε	λ_{em} [1]	Φ_F [2]
		Dibenzofuran series		
5b	289	4.13	355	0.06
12b	286	4.39	354	0.01
17b	289	4.35	401	0.02
1ba	305, 317, 343	4.44, 4.37, 4.15	392	0.03
1bb	296, 307, 321, 348	4.03, 4.14, 4.14, 3.87	417	0.01
2b	287, 341	4.50, 4.16	386	0.03
		Pyrene series		
6	278, 345	4.45, 4.37	391	0.18
13	268, 278, 331, 346	4.52, 4.61, 4.34, 4.49	388	0.01
18	268, 279, 330, 346	4.43, 4.57, 4.25, 4.37	411	0.42
3	288, 346, 381, 402, 440	4.46, 4.65, 4.18, 4.26, 3.50	457	0.05
		Dibenzothiophene series		
5c	287, 301, 330	3.98, 3.71, 3.56	373	0.02
12c	288, 330	4.11, 3.61	394	0.02
17c	287, 310, 402	4.46, 4.45, 3.59	420	0.01
1ca	279, 293, 318, 343, 386	4.21, 4.32, 4.39, 3.99, 3.71	402	0.02
1cb	321, 357, 391	4.29, 3.91, 3.68	434	0.01
2c	298, 353, 390	4.70, 4.17, 3.80	399	0.02
		Carbazole series		
5a	265, 295, 349	4.24, 3.96, 3.58	372	0.10
		Dibenzofuran series		
12a	264, 296, 351	4.47, 4.10, 3.71	371	0.01
17a	264, 296, 350	4.45, 4.30, 3.68	415	0.03
1aa	321, 343, 348, 361, 397	4.53, 4.02, 4.01, 4.01, 3.90	413	0.03
1ab	325, 402	4.54, 3.91	439	0.01
1ac	319, 343, 358, 376, 396	4.51, 4.01, 4.04, 3.84, 3.92	408	0.03
2a	305, 359, 380, 400	4.73, 4.03, 3.77, 3.75	414	0.08
		Spirobifluorene series		
7	300, 309	4.01, 4.06	363	0.06
14	297, 309	4.09, 4.13	364	0.02
19	297, 309	4.33, 4.35	399	0.03
4	279, 298, 310, 322, 356	4.57, 4.56, 4.46, 4.54, 4.22	417	0.03

[1] λ_{abs}, λ_{em} are reported in nm. All photophysical values reflect the average of three independent measurements. [2] Φ_F was measured referring to quinine sulfate as the standard (Φ_{STD} = 0.546 in H_2SO_4 0.5 M, λ_{ex} 366 nm) [72].

The conjugation extension from **5a** to the final thiahelicenes **1aa**, **1ab**, **1ac**, and **2a** led to a significant red-shift of the optical features. Although there was no absorption for **5a** over 375 nm, all of the above-mentioned thiahelicenes showed an extended absorption band up to 425 nm. The fluorescence spectra reflected the same behavior, with the **5a** maximum at 372 nm red-shifted around 440 nm for the thiahelicene hybrid systems. The effect of the substituents on the helical skeleton was also investigated. Benzo fused derivative **2a** showed a negligible shift when compared to **1aa**, which bears two phenyl groups on the core. The replacement of one phenyl ring with an ethyl chain in the asymmetric **1ac** leads to a small 5 nm blue shift of emission maximum, while the introduction of electron-rich thienyl substituents results in the red-shifted properties of **1ab**, along with a decrease in the quantum yield. This overall trend was confirmed by investigating the other hybrid systems, whose UV–Vis and fluorescence spectra are reported in the Supplementary Materials (Figure S3a–d). As an example, the above-mentioned red-shifting effect caused by the introduction of two electron-rich thienyl groups could be likewise observed in the dibenzofuran and the dibenzothiophene families, where compounds **1bb** and **1cb** showed the most bathochromic emission within their series ($\lambda_{em\ max}$ = 417 and 434 nm,

respectively). Figure 5b highlights the effects of different heterocycles along the helix, when the substituents are two pending phenyl groups. Pyrene hybrid **3** was the most red-shifted and emissive system, in accordance with previous results on helicene-based analogues [19]. Since **1aa**, **1ba**, and **1ca** showed an equivalent extended π-surface, their photophysical features relied on the heteroatom: emissive bathochromic shifts from X = O (**1ba**, $\lambda_{em\ max}$ = 392 nm) to X = S (**1ca**, $\lambda_{em\ max}$ = 402 nm) and, finally, to N-CH_3 (**1aa**, $\lambda_{em\ max}$ = 413 nm) were observed, in agreement with the aromatic character of the heterocycles [73,74]. The same trend could be identified looking at the absorption spectra: while **1ba** showed no absorption after 380 nm, **1ca** and **1aa** had an absorption shoulder at 386 nm and 397 nm, respectively. Finally, spirobifluorene-derivative **4** displayed an intermediate behavior, with the emission maximum and an absorption tail at 417 and 356 nm, respectively.

3. Materials and Methods

3.1. General Methods

Organic and inorganic reagents and solvents obtained from commercial sources were used as received unless otherwise stated. Solutions of *n*BuLi (1.6 M in hexane) were purchased from Aldrich and titrated prior to use. Bromides **9b**, **9c**, **10**, and **11** were purchased from TCI. Bromide **9a** was synthesized through the methylation of commercial 4-bromocarbazole with methyl iodide according to the literature [57]. The outcome of the reactions was monitored by thin-layer chromatography (TLC) on silica gel 60 F254 precoated plates. Column chromatography was performed on silica gel 60 (70–230 mesh). Melting points were recorded with a Büchi Melting Point B-540 apparatus and uncorrected. The IR spectra were registered on powders using an ATR Fourier transform infrared (FTIR) spectrometer (PerkinElmer spectrum 100). High-resolution mass spectra (HRMS) were recorded with an electron ionization (EI) spectrometer (FISONS-Vg Autospec-M246). The HRMS spectrum for compound **4** was recorded by means of laser desorption/ionization (LDI) using a MALDI-TOF/TOF Autoflex III-Bruker Daltonics.

NMR experiments were performed at 298 K on a Bruker Avance 600 MHz spectrometer. The NMR experiments were carried out in 500 µL of $CDCl_3$ using about 20 mg of sample (in some case a lower quantity around 2 mg must be used due to low solubility). Proton and carbon chemical shifts were assigned unambiguously using mono- and bi-dimensional experiments from the standard Bruker library, and the assignments are reported in Tables S1–S27 (see SM). For ^{1}H spectra, 1D sequence with 30 degree flip angle was used while the APT (attached proton test, J-modulated spin-echo) sequence allowed the ^{13}C analysis and the determination of the number of attached protons (according to the sequence, C and CH_2 are phased positive and CH and CH_3 negative). For the identification of 2D homonuclear shift correlation, COSY spectra with gradient pulses were acquired using four scans and 128 increments. ^{1}H-^{13}C HSQC experiments were acquired via double inept transfer using Echo/Antiecho gradient selection with eight scans and 256 increments. ^{1}H-^{13}C HMBC spectra were obtained via heteronuclear zero and double quantum coherence, with 16 scans and 256 increments. For the identification of long-range couplings, a *J* value of 10 Hz was used and a low-pass *J*-filter (*J* = 145 Hz) was applied to suppress one-bond correlations. Where necessary to solve ambiguity, phase sensitive 2D-NOESY experiments with gradient pulses in mixing time were performed with a mixing time of 500 ms with 16 scans and 256 increments.

Absorption and emission spectra were measured in CH_2Cl_2 for all the compounds tested. Stock solutions were prepared in CH_2Cl_2 with a concentration between 2.2×10^{-3} M and 8.5×10^{-3} M for all the compounds tested. The sample concentration was adjusted to have an absorbance between 0.1 and 1 at the $\lambda_{abs\ max}$ to evaluate the general photophysical properties in CH_2Cl_2 (molar extinction coefficient reported as log ε, $\lambda_{abs\ max}$, and $\lambda_{em\ max}$). All measurements were carried out in a 1 cm four-sided quartz cuvette from Hellma Analitics. Absorption spectra were measured on a Shimadzu UV-1900i UV–Vis spectrophotometer using a resolution of 0.5 nm. Steady state emission spectra were measured on a Shimadzu RF-6000. The excitation and the emission slits were set at five

and 10 nm respectively, while the resolution was 1 nm. All the absorption and steady state emission spectra were corrected for their respective blank.

Fluorescence quantum yield evaluation. The sample concentrations were adapted to have an absorbance lower than 0.1 at the excitation wavelength (λ_{ex}) using the above-mentioned stock solutions. The fluorescence quantum yields (Φ_F) were evaluated compared to an external standard, quinine sulfate (Φ_{STD} = 0.546 in H_2SO_4 0.5 M, λ_{ex} 366 nm) [72], by applying the following equation.

$$\Phi_F = \Phi_{STD} \frac{I}{I_{STD}} \frac{Abs_{STD}}{Abs} \frac{n^2}{n^2_{STD}}$$

where Φ_{STD} is the fluorescence quantum yield of the standard; and I and I_{STD} are the integrated area of the emission band of the sample and the standard, respectively. Abs and Abs_{STD} are the absorbance at the excitation wavelength for the sample and the standard, respectively. n and n_{STD} are the solvent refractive index of the sample and the standard solutions, respectively.

3.2. General Procedure for the Synthesis of Benzothiophene-Based Biaryls **5a–c**, **6**, *and* **7**

A degassed mixture of bromide **9a–c**, **10**, or **11** (1.5 mmol), 1-benzothien-3-ylboronic acid (**8**) (373.8 mg, 2.1 mmol), $Pd(PPh_3)_4$ (173 mg, 0.15 mmol), and Cs_2CO_3 (684 mg, 2.1 mmol) in dry DMF (5 mL) was stirred at 80 °C under a nitrogen atmosphere for 8–11 h. After completion of the reaction, the mixture was cooled to room temperature, diluted with CH_2Cl_2, and poured into water (50 mL). The aqueous phase was extracted with CH_2Cl_2 (3 × 20 mL). The collected organic phases were washed with water (3 × 30 mL), dried over Na_2SO_4, and concentrated under reduced pressure. The crude was purified by column chromatography on silica gel to give the products **5a–c**, **6**, or **7**.

3.3. General Procedure for the Synthesis of Iodides **12a–c**, **13** *and* **14**

A solution of *n*BuLi (1.41 mL, 2.25 mmol, 1.6 M in hexane) was added dropwise to a stirring solution of biaryl **5a–c**, **6**, or **7** (1.5 mmol) in dry THF (2 mL for **5a–c**, 16 mL for **6** or **7**) at −50 °C under an argon atmosphere. The resulting mixture was stirred for 1 h at −50 °C. A solution of I_2 in THF (2.25 mL, 2.25 mmol, 1 M) was added dropwise to the mixture. After 15 min, the mixture was warmed to room temperature and stirred overnight. A saturated aqueous solution of $Na_2S_2O_3$ (20 mL) was slowly added, and the aqueous phase was extracted with CH_2Cl_2 (3 × 20 mL). The collected organic phases were washed with water (2 × 20 mL), dried over Na_2SO_4, and concentrated under reduced pressure. The crude products **12a–c**, **13**, or **14** were washed with diethyl ether and pentane and used in the next steps without further purification.

3.4. General Procedure for the Carboannulation of Alkynes **15a–c** *with Iodides* **12a–c**, **13**, *and* **14**

A degassed mixture of iodides **12a–c**, **13**, or **14** (0.1 mmol), alkyne **15a–c** (0.15 mmol), $Pd(OAc)_2$ (1.12 mg, 0.005 mmol), NaOAc (16.4 mg, 0.2 mmol), LiCl (4.2 mg, 0.1 mmol) in dry DMF (1 mL) was stirred at 100 °C under an argon atmosphere for 9 h. After completion of the reaction, the mixture was cooled to room temperature, diluted with CH_2Cl_2, and added to water (10 mL). The aqueous phase was extracted with CH_2Cl_2 (5 × 5 mL) and the collected organic phases were washed with water (3 × 10 mL), dried over Na_2SO_4, and concentrated under reduced pressure. The crude was purified by column chromatography on silica gel to give the products **1aa**, **1ab**, **1ac**, **1ba**, **1bb**, **1ca**, **1cb**, **3**, or **4**.

3.5. General Procedure for the Synthesis of Intermediates **17a–c**, **18**, *and* **19**

A degassed mixture of iodide **12a–c**, **13**, or **14** (0.4 mmol), phenylboronic acid (**16**) (0.8 mmol), $PdCl_2$(dppf) (29 mg, 0.04 mmol), KF (70 mg, 1.2 mmol) in toluene (10 mL) and methanol (10 mL) was stirred at 70 °C under a nitrogen atmosphere for 9 h. After completion of the reaction, the mixture was cooled to room temperature and the solvent was removed under reduced pressure. The residue was diluted with CH_2Cl_2 and poured into

water (40 mL). The aqueous phase was extracted with CH_2Cl_2 (5 × 20 mL) and the collected organic phases were dried over Na_2SO_4, and concentrated under reduced pressure. The crude was purified by column chromatography on silica gel to afford the products **17a–c**, **18**, or **19**.

3.6. General Procedure for the Synthesis of Benzo Fused Thiahelicenes **2a–c**

A solution of **17a–c** (0.16 mmol) and iodine (0.096 mmol) in cyclohexane (750 mL) was stirred at room temperature and irradiated with a 125 W unfiltered medium-pressure Hg lamp. After the complete conversion of the starting material, the solvent was removed under vacuum, and the residue was dissolved in CH_2Cl_2 (30 mL) and the organic phase was washed with a saturated aqueous solution of $Na_2S_2O_3$ (2 × 15 mL), dried over Na_2SO_4, and concentrated under reduced pressure. The crude was purified by column chromatography on silica gel to afford the products **2a–c**.

4. Conclusions

In summary, we report here the synthesis of a novel class of thiahelicenes **1**, **3**, and **4**, all containing a benzothiophene subunit and a second heteroatom such as nitrogen and oxygen, embedded in the helix, or a pyrene or a spirobifluorene moiety. These new helical systems are obtained through a straightforward and general three-step procedure starting from easily available and/or commercial starting materials. It is noteworthy that the key intermediates **12–14** are smoothly obtained in excellent yields by means of a two-step synthesis involving Suzuki coupling between bromides **9**−**11** and boronic acid **8** (92–98%), followed by the iodination of bi(hetero)aryls **5–7** (84–92%). The palladium-catalyzed annulation of internal alkynes **15** with iodides **12–14** provides a small library of functionalized thiahelicenes **1**, **3**, and **4** including heterohelicenes containing two different heteroatoms (i.e., aza-thiahelicenes **1aa–1ac**, oxa-thiahelicenes **1ba–1bb**) and pyrene- and spirobifluorene-hybrids **3** and **4**.

Additionally, we applied the iodide key precursors **12a**−**c** to synthesize the benzo fused compounds **2a**−**c** by means of two simple synthetic steps: an efficient Suzuki coupling between the iodides and the phenylboronic acid (**16**), followed by the photocyclization of intermediates **17a**−**c**.

Both experimental and theoretical studies on the configurational stability of thia[6]helicenes **1** and **2** confirmed their stability toward racemization at room temperature, while the pyrene-based thia[5]helicene **3** was found to be unstable, as somehow expected for other [5]helicenes. Moreover, the configuration assignment for the benzo fused thiahelicene **2a** was unequivocally established by means of the comparison between experimental CD spectra and those obtained with DFT calculations.

Finally, the photophysical characters of both thiahelicenes and the corresponding intermediates were systematically evaluated to provide a complete overview on the new molecules proposed in this work. The obtained data showed regular trends in all the thiahelicenes series synthesized with spectroscopic traits, in line with those previously observed for similar heterohelicenes.

This study offers an important breakthrough in helicene chemistry, and the substrate scope of these protocols could indeed be extended thanks to the great availability of commercial or easy to synthesize alkynes and (hetero) arylboronic acids, with the clear perspective to produce, through a few low-cost reaction steps, new classes of heterohelicenes. Those here reported thiahelicenes also represent a useful platform from which different heterohelicenes could be prepared by downstream modification of the sulfur atoms. Thus, further studies will be devoted to applying this methodology to other classes of heterohelicenes with potential novel and enhanced functional properties.

Supplementary Materials: The following supporting information can be downloaded at: https://www.mdpi.com/article/10.3390/catal12040366/s1, Scheme S1: Suzuki coupling between **8** and **9c** with 5 mol% of $Pd(PPh_3)_4$; characterization, ^1H and ^{13}C NMR spectra of new compounds; Tables S1–S27: ^1H and ^{13}C NMR assignment; Table S28: HPLC analyses data; HPLC chromatograms

of compounds **1aa**, **2a**, **2b**, **2c**, and **3**. Figure S1: Definition of τ and φ dihedral angles; Figure S2: Experimental and calculated CD spectra of **2a**; Figure S3: Absorption and emission spectra in CH_2Cl_2 of different series. ^{1}H-^{13}C HSQC spectra of new compounds. (References [75–80] are cited in the Supplementary Materials).

Author Contributions: Conceptualization, S.C. and E.L.; Methodology, V.P., C.V., A.R. and F.V. conceived and performed NMR experiments; Software, G.L. for DFT calculations; Validation, G.L., S.A. and C.G.; Formal analysis, F.C.; Investigation, F.C., V.P., C.G. and G.R.; Resources, E.L.; Data curation, G.R., A.F. and F.C.; Writing—original draft preparation, S.C. and C.G.; Writing—review and editing, S.C., F.C., E.L., G.L., S.A., G.M., C.G., A.F., G.V. and V.P.; Supervision, S.C., F.C. and E.L.; Project administration, S.C. and E.L.; Funding acquisition, E.L., S.C., G.L. and S.A. All authors have read and agreed to the published version of the manuscript.

Funding: S.C. thanks Università degli Studi di Milano for the financial support (Piano di Sostegno alla Ricerca 2015/2017-Linea 2, Azione A-Giovani Ricercatori). S.A. and G.L. thank Support from the Italian MIUR (PRIN 2017, project "Physico-chemical Heuristic Approaches: Nanoscale Theory of Molecular Spectroscopy" (PHANTOMS), prot. 2017A4XRCA).

Acknowledgments: The authors thank Natale Crisafulli and Cristina Gabbrielli for some of the experimental work. V.P. thanks Università degli Studi di Milano for the Ph.D. fellowship. Mass LDI spectrometry analysis was performed at the Mass Spectrometry facility of the Unitech COSPECT at the Università degli Studi di Milano. S.A. and G.L. acknowledge support from Big&Open Data Innovation Laboratory (BODaI-Lab), University of Brescia, granted by Fondazione Cariplo and Regione Lombardia and Computing Center CINECA (Bologna), Italy.

Conflicts of Interest: The authors declare no conflict of interest.

References

1. Ravat, P. Carbo[n]helicenes Restricted to Enantiomerize: An Insight into the Design Process of Configurationally Stable Functional Chiral PAHs. *Chem. Eur. J.* **2021**, *27*, 3957–3967. [PubMed]
2. Chen, C.-F.; Shen, Y. *Helicene Chemistry, from Synthesis to Applications*; Springer: Berlin/Heidelberg, Germany, 2017.
3. Shen, Y.; Chen, C.-F. Helicenes: Synthesis and Applications. *Chem. Rev.* **2012**, *112*, 1463–1535. [PubMed]
4. Nakai, Y.; Mori, T.; Inoue, Y. Theoretical and Experimental Studies on Circular Dichroism of Carbo[n]helicenes. *J. Phys. Chem. A* **2012**, *116*, 7372–7385. [PubMed]
5. Zhao, W.-L.; Li, M.; Lu, H.-Y.; Chen, C.-F. Advances in helicene derivatives with circularly polarized luminescence. *Chem. Commun.* **2019**, *55*, 13793–13803.
6. Dhbaibi, K.; Favereau, L.; Crassous, J. Enantioenriched Helicenes and Helicenoids Containing Main-Group Elements (B, Si, N, P). *Chem. Rev.* **2019**, *119*, 8846–8953.
7. Pop, F.; Zigon, N.; Avarvari, N. Main-Group-Based Electro- and Photoactive Chiral Materials. *Chem. Rev.* **2019**, *119*, 8435–8478.
8. Biet, T.; Martin, K.; Hankache, J.; Hellou, N.; Hauser, A.; Bürgi, T.; Vanthuyne, N.; Aharon, T.; Caricato, M.; Crassous, J.; et al. Triggering Emission with the Helical Turn in Thiadiazole-Helicenes. *Chem. Eur. J.* **2017**, *23*, 437–446.
9. Mori, T. Chiroptical Properties of Symmetric Double, Triple, and Multiple Helicenes. *Chem. Rev.* **2021**, *121*, 2373–2412.
10. Li, C.; Yang, Y.; Miao, Q. Recent Progress in Chemistry of Multiple Helicenes. *Chem. Asian J.* **2018**, *13*, 884–894.
11. Swain, A.K.; Radacki, K.; Braunschweig, H.; Ravat, P. Pyrene-Fused [7]Helicenes Connected Via Hexagonal and Heptagonal Rings: Stereospecific Synthesis and Chiroptical Properties. *J. Org. Chem.* **2022**, *87*, 993–1000.
12. Swain, A.k.; Kolanji, K.; Stapper, C.; Ravat, P. C2- and C1-Symmetric Configurationally Stable Pyrene-Fused [5]Helicenes Connected via Hexagonal and Heptagonal Rings. *Org. Lett.* **2021**, *23*, 1339–1343. [PubMed]
13. Wang, L.; Han, Y.; Zhang, J.; Li, X.; Liu, X.; Xiao, J. Stable Double and Quadruple [5]Helicene Derivatives: Synthesis, Structural Analysis, and Physical Properties. *Org. Lett.* **2020**, *22*, 261–264. [PubMed]
14. Hu, Y.; Paternò, G.M.; Wang, X.-Y.; Wang, X.-C.; Guizzardi, M.; Chen, Q.; Schollmeyer, D.; Cao, X.-Y.; Cerullo, G.; Scotognella, F.; et al. π-Extended Pyrene-Fused Double [7]Carbohelicene as a Chiral Polycyclic Aromatic Hydrocarbon. *J. Am. Chem. Soc.* **2019**, *141*, 12797–12803. [PubMed]
15. Bam, R.; Yang, W.; Longhi, G.; Abbate, S.; Lucotti, A.; Tommasini, M.; Franzini, R.; Villani, C.; Catalano, V.J.; Olmstead, M.M.; et al. Four-Fold Alkyne Benzannulation: Synthesis, Properties, and Structure of Pyreno[a]pyrene-Based Helicene Hybrids. *Org. Lett.* **2019**, *21*, 8652–8656.
16. Wang, C.-Z.; Kihara, R.; Feng, X.; Thuéry, P.; Redshaw, C.; Yamato, T. Synthesis, Structure and Photophysical Properties of Pyrene–based [5]Helicenes: An Experimental and Theoretical Study. *ChemistrySelect* **2017**, *2*, 1436–1441.
17. Buchta, M.; Rybáček, J.; Jančařík, A.; Kudale, A.A.; Buděšínský, M.; Chocholoušová, J.V.; Vacek, J.; Bednárová, L.; Císařová, I.; Bodwell, G.J.; et al. Chimerical Pyrene-Based [7]Helicenes as Twisted Polycondensed Aromatics. *Chem. Eur. J.* **2015**, *21*, 8910–8917.

18. Bock, H.; Subervie, D.; Mathey, P.; Pradhan, A.; Sarkar, P.; Dechambenoit, P.; Hillard, E.A.; Durola, F. Helicenes from Diarylmaleimides. *Org. Lett.* **2014**, *16*, 1546–1549.
19. Hu, J.-Y.; Feng, X.; Paudel, A.; Tomiyasu, H.; Rayhan, U.; Thuéry, P.; Elsegood, M.R.J.; Redshaw, C.; Yamato, T. Synthesis, Structural, and Photophysical Properties of the First Member of the Class of Pyrene-Based [4]Helicenes. *Eur. J. Org. Chem.* **2013**, *2013*, 5829–5837.
20. Hu, J.-Y.; Paudel, A.; Seto, N.; Feng, X.; Era, M.; Matsumoto, T.; Tanaka, J.; Elsegood, M.R.J.; Redshaw, C.; Yamato, T. Pyrene-cored blue-light emitting [4]helicenes: Synthesis, crystal structures, and photophysical properties. *Org. Biomol. Chem.* **2013**, *11*, 2186–2197.
21. Bédard, A.-C.; Vlassova, A.; Hernandez-Perez, A.C.; Bessette, A.; Hanan, G.S.; Heuft, M.A.; Collins, S.K. Synthesis, Crystal Structure and Photophysical Properties of Pyrene–Helicene Hybrids. *Chem. Eur. J.* **2013**, *19*, 16295–16302.
22. Hayward, R.J.; Hopkinson, A.C.; Leznoff, C.C. Photocyclization reactions of aryl polyenes—VI: The photocyclization of 1,4-diaryl-1,3-butadienes. *Tetrahedron* **1972**, *28*, 439–447.
23. Vingiello, F.A.; Henson, P.D. 7-Phenyldibenz[a,h]anthracene and Benzo[e]naphtho[1,2-b]pyrene1,2. *J. Org. Chem.* **1965**, *30*, 2842–2845.
24. Stara, I.; Stary, I. Helically chiral aromatics: The synthesis of helicenes by [2+2+2] cycloisomerization of π-electron system. *Acc. Chem. Res.* **2020**, *53*, 144–158.
25. Tanaka, K.; Kimura, Y.; Murayama, K. Enantioselective helicene synthesis by rhodium-catalyzed [2+2+2] cycloadditions. *Bull. Chem. Soc. Jpn.* **2015**, *88*, 375–385.
26. Hoffmann, N. Photochemical reactions applied to the synthesis of helicenes and helicene-like compounds. *J. Photochem. Photobiol. C* **2014**, *19*, 1–19.
27. Kaga, A.; Iida, H.; Tsuchiya, S.; Saito, H.; Nakano, K.; Yorimitsu, H. Aromatic Metamorphosis of Thiophenes by Means of Desulfurative Dilithiation. *Chem. Eur. J.* **2021**, *27*, 4567–4572. [PubMed]
28. Matsuo, Y.; Tanaka, T.; Osuka, A. Diazadimethano[8]circulene: Synthesis, Structure, Properties, and Isolation of Stable Radical Cation. *Chem. Lett.* **2020**, *49*, 959–962.
29. Takase, K.; Noguchi, K.; Nakano, K. Synthesis of Pyrrole-Containing Chiral Spiro Molecules and Their Optical and Chiroptical Properties. *Bull. Chem. Soc. Jpn.* **2019**, *92*, 1008–1017.
30. Nagata, Y.; Kato, S.; Miyake, Y.; Shinokubo, H. Synthesis of Tetraaza[8]circulenes from Tetrathia[8]circulenes through an SNAr-Based Process. *Org. Lett.* **2017**, *19*, 2718–2721.
31. Yorimitsu, H.; Vasu, D.; Bhanuchandra, M.; Murakami, K.; Osuka, A. Aromatic Metamorphosis of Dibenzothiophenes. *Synlett* **2016**, *27*, 1765–1774.
32. Uematsu, K.; Hayasaka, C.; Takase, K.; Noguchi, K.; Nakano, K. Transformation of Thia[7]helicene to Aza[7]helicenes and [7]Helicene-like Compounds via Aromatic Metamorphosis. *Molecules* **2022**, *27*, 606. [PubMed]
33. Yanagi, T.; Tanaka, T.; Yorimitsu, H. Asymmetric systematic synthesis, structures, and (chir)optical properties of a series of dihetero[8]helicenes. *Chem. Sci.* **2021**, *12*, 2784–2793. [PubMed]
34. Licandro, E.; Cauteruccio, S.; Dova, D. Thiahelicenes: From basic knowledge to applications. *Adv. Heteroc. Chem.* **2016**, *118*, 1–46.
35. Collins, S.K.; Vachon, M.P. Unlocking the potential of thiaheterohelicenes: Chemical synthesis as the key. *Org. Biomol. Chem.* **2006**, *4*, 2518–2524.
36. Champagne, B.; Labidi, S.N. Second-order nonlinear optical responses of heptahelicene and heptathiahelicene derivatives. *Chem. Phys. Lett.* **2016**, *644*, 195–200.
37. Bossi, A.; Licandro, E.; Maiorana, S.; Rigamonti, C.; Righetto, S.; Stephenson, G.R.; Spassova, M.; Botek, E.; Champagne, B. Theoretical and Experimental Investigation of Electric Field Induced Second Harmonic Generation in Tetrathia[7]helicenes. *J. Phys. Chem. C* **2008**, *112*, 7900–7907.
38. Botek, E.; André, J.-M.; Champagne, B.; Verbiest, T.; Persoons, A. Mixed electric-magnetic second-order nonlinear optical response of helicenes. *J. Chem. Phys.* **2005**, *122*, 234713.
39. Botek, E.; Spassova, M.; Champagne, B.; Asselberghs, I.; Persoons, A.; Clays, K. Hyper-Rayleigh scattering of neutral and charged helicenes. *Chem. Phys. Lett.* **2005**, *412*, 274–279.
40. Champagne, B.; André, J.-M.; Botek, E.; Licandro, E.; Maiorana, S.; Bossi, A.; Clays, K.; Persoons, A. Theoretical Design of Substituted Tetrathia-[7]-Helicenes with Large Second-Order Nonlinear Optical Responses. *ChemPhysChem* **2004**, *5*, 1438–1442.
41. Daul, C.A.; Ciofini, I.; Weber, V. Investigation of NLO properties of substituted (M)-tetrathia-[7]-helicenes by semiempirical and DFT methods. *Int. J. Quantum Chem.* **2003**, *91*, 297–302.
42. Fukumi, T.; Sakaguchi, T.; Miya, M.; Nakagawa, H.; Yamada, K.-I.; Kawazura, H. Determination of Second Molecular Hyperporalizability γ of Thiaheterohelicene by Degenerate Four-Wave Mixing Method. *Rev. Laser Eng.* **1994**, *22*, 409–414.
43. Chaunchaiyakul, S.; Krukowski, P.; Tsuzuki, T.; Minagawa, Y.; Akai-Kasaya, M.; Saito, A.; Osuga, H.; Kuwahara, Y. Self-Assembly Formation of M-Type Enantiomer of 2,13-Bis(hydroxymethyl)[7]-thiaheterohelicene Molecules on Au(111) Surface Investigated by STM/CITS. *J. Phys. Chem. C* **2015**, *119*, 21434–21442.
44. Krukowski, P.; Chaunchaiyakul, S.; Akai-Kasaya, M.; Saito, A.; Osuga, H.; Kuwahara, Y. Adsorption and Light Emission of a Racemic Mixture of [7]thiaheterohelicene-2,13-carboxaldehyde on Au(111), Cu(001), and NiAl(110) Surfaces Investigated Using a Scanning Tunneling Microscope. *J. Phys. Chem. C* **2021**, *125*, 9419–9427.

45. Nakamura, T.; Kondoh, H.; Matsumoto, M. Scanning Tunneling Microscopy Observations of [7]Thiahelicene Adsorbed on Au(111). *Mol. Cryst. Liq. Cryst.* **1999**, *337*, 273–276.
46. Arnaboldi, S.; Cauteruccio, S.; Grecchi, S.; Benincori, T.; Marcaccio, M.; Biroli, A.O.; Longhi, G.; Licandro, E.; Mussini, P.R. Thiahelicene-based inherently chiral films for enantioselective electroanalysis. *Chem. Sci.* **2019**, *10*, 1539–1548.
47. Dova, D.; Viglianti, L.; Mussini, P.R.; Prager, S.; Dreuw, A.; Voituriez, A.; Licandro, E.; Cauteruccio, S. Tetrathia[7]helicene Phosphorus Derivatives: Experimental and Theoretical Investigations of Electronic Properties, and Preliminary Applications as Organocatalysts. *Asian J. Org. Chem.* **2016**, *5*, 537–549.
48. Cauteruccio, S.; Dova, D.; Benaglia, M.; Genoni, A.; Orlandi, M.; Licandro, E. Synthesis, Characterisation, and Organocatalytic Activity of Chiral Tetrathiahelicene Diphosphine Oxides. *Eur. J. Org. Chem.* **2014**, *2014*, 2694–2702.
49. Cauteruccio, S.; Loos, A.; Bossi, A.; Blanco Jaimes, M.C.; Dova, D.; Rominger, F.; Prager, S.; Dreuw, A.; Licandro, E.; Hashmi, A.S.K. Gold(I) Complexes of Tetrathiaheterohelicene Phosphanes. *Inorg. Chem.* **2013**, *52*, 7995–8004.
50. Monteforte, M.; Cauteruccio, S.; Maiorana, S.; Benincori, T.; Forni, A.; Raimondi, L.; Graiff, C.; Tiripicchio, A.; Stephenson, G.R.; Licandro, E. Tetrathiaheterohelicene Phosphanes as Helical-Shaped Chiral Ligands for Catalysis. *Eur. J. Org. Chem.* **2011**, *2011*, 5649–5658.
51. Taroni, T.; Cauteruccio, S.; Vago, R.; Franchi, S.; Barbero, N.; Licandro, E.; Ardizzone, S.; Meroni, D. Thiahelicene-grafted halloysite nanotubes: Characterization, biological studies and pH triggered release. *Appl. Surf. Sci.* **2020**, *520*, 146351.
52. Cauteruccio, S.; Bartoli, C.; Carrara, C.; Dova, D.; Errico, C.; Ciampi, G.; Dinucci, D.; Licandro, E.; Chiellini, F. A Nanostructured PLGA System for Cell Delivery of a Tetrathiahelicene as a Model for Helical DNA Intercalators. *ChemPlusChem* **2015**, *80*, 490–493. [PubMed]
53. Shinohara, K.-I.; Sannohe, Y.; Kaieda, S.; Tanaka, K.-I.; Osuga, H.; Tahara, H.; Xu, Y.; Kawase, T.; Bando, T.; Sugiyama, H. A Chiral Wedge Molecule Inhibits Telomerase Activity. *J. Am. Chem. Soc.* **2010**, *132*, 3778–3782. [PubMed]
54. Xu, Y.; Zhang, Y.X.; Sugiyama, H.; Umano, T.; Osuga, H.; Tanaka, K. (P)-Helicene Displays Chiral Selection in Binding to Z-DNA. *J. Am. Chem. Soc.* **2004**, *126*, 6566–6567.
55. Nakagawa, H.; Gomi, K.; Yamada, K.-I. Chiral Recognition of Thiaheterohelicenes by Alkyl beta;-D-Pyranoside Micelles. Influence of Extension of Helix. *Chem. Pharm. Bull.* **2001**, *49*, 49–53.
56. Pelliccioli, V.; Dova, D.; Baldoli, C.; Graiff, C.; Licandro, E.; Cauteruccio, S. Diversified Syntheses of Tetrathia[7]helicenes by Metal-Catalyzed Cross-Coupling Reactions. *Eur. J. Org. Chem.* **2021**, *2021*, 383–395.
57. Shen, D.; Xu, Y.; Shi, S.-L. A Bulky Chiral N-Heterocyclic Carbene Palladium Catalyst Enables Highly Enantioselective Suzuki–Miyaura Cross-Coupling Reactions for the Synthesis of Biaryl Atropisomers. *J. Am. Chem. Soc.* **2019**, *141*, 14938–14945.
58. Schubert, M.; Trosien, S.; Schulz, L.; Brandscheid, C.; Schollmeyer, D.; Waldvogel, S.R. Oxidative (Cross-)Coupling Reactions Mediated by C–H Activation of Thiophene Derivatives by Using Molybdenum(V) Reagents. *Eur. J. Org. Chem.* **2014**, *2014*, 7091–7094.
59. Worlikar, S.A.; Larock, R.C. Pd-catalyzed Reactions Involving Arynes. *Curr. Org. Chem.* **2011**, *15*, 3214–3232.
60. Larock, R.C. Palladium-Catalyzed Annulation of Alkynes. In *Palladium in Organic Synthesis*; Tsuji, J., Ed.; Springer GmbH: Berlin/Heidelberg, Germany, 2005; pp. 147–182.
61. Larock, R.C.; Doty, M.J.; Tian, Q.; Zenner, J.M. Synthesis of Polycyclic Aromatic Hydrocarbons by the Pd-Catalyzed Annulation of Alkynes. *J. Org. Chem.* **1997**, *62*, 7536–7537.
62. Larock, R.C.; Yum, E.K. Synthesis of indoles via palladium-catalyzed heteroannulation of internal alkynes. *J. Am. Chem. Soc.* **1991**, *113*, 6689–6690.
63. Larock, R.C.; Yum, E.K.; Doty, M.J.; Sham, K.K.C. Synthesis of Aromatic Heterocycles via Palladium-Catalyzed Annulation of Internal Alkynes. *J. Org. Chem.* **1995**, *60*, 3270–3271.
64. Larock, R.C.; Doty, M.J.; Cacchi, S. Synthesis of indenones via palladium-catalyzed annulation of internal alkynes. *J. Org. Chem.* **1993**, *58*, 4579–4583.
65. Bossi, A.; Maiorana, S.; Graiff, C.; Tiripicchio, A.; Licandro, E. Silyl-Substituted Tetrathia[7]helicenes: Synthesis, X-ray Characterization and Reactivity. *Eur. J. Org. Chem.* **2007**, *2007*, 4499–4509.
66. Dova, D.; Cauteruccio, S.; Prager, S.; Dreuw, A.; Graiff, C.; Licandro, E. Chiral Thiahelicene-Based Alkyl Phosphine–Borane Complexes: Synthesis, X-ray Characterization, and Theoretical and Experimental Investigations of Optical Properties. *J. Org. Chem.* **2015**, *80*, 3921–3928. [PubMed]
67. Bossi, A.; Falciola, L.; Graiff, C.; Maiorana, S.; Rigamonti, C.; Tiripicchio, A.; Licandro, E.; Mussini, P.R. Electrochemical activity of thiahelicenes: Structure effects and electrooligomerization ability. *Electrochim. Acta* **2009**, *54*, 5083–5097.
68. Grimme, S.; Peyerimhoff, S.D. Theoretical study of the structures and racemization barriers of [n]helicenes (n = 3–6, 8). *Chem. Phys.* **1996**, *204*, 411–417.
69. Lebon, F.; Longhi, G.; Gangemi, F.; Abbate, S.; Priess, J.; Juza, M.; Bazzini, C.; Caronna, T.; Mele, A. Chiroptical Properties of Some Monoazapentahelicenes. *J. Phys. Chem. A* **2004**, *108*, 11752–11761.
70. Hua, W.; Liu, Z.; Duan, L.; Dong, G.; Qiu, Y.; Zhang, B.; Cui, D.; Tao, X.; Cheng, N.; Liu, Y. Deep-blue electroluminescence from nondoped and doped organic light-emitting diodes (OLEDs) based on a new monoaza[6]helicene. *RSC Adv.* **2015**, *5*, 75–84.
71. Kaiser, J.; Mekic, A.; Parham, A.H.; Buchholz, H.; König, B. Synthesis and Characterization of Naphtho[2,1-b:7,8-b′]bis[1]benzothiophene. *Eur. J. Org. Chem.* **2020**, *2020*, 66–69.
72. Brouwer, A.M. Standards for photoluminescence quantum yield measurements in solution. *Pure Appl. Chem.* **2011**, *83*, 2213–2228.

73. Carmody, M.P.; Cook, M.J.; Tack, R.D. Aromaticity and tautomerism—V: The basicity and aromaticity of pyrrole, furan, thiophen and their benzo derivatives. *Tetrahedron* **1976**, *32*, 1767–1771.
74. Horner, K.E.; Karadakov, P.B. Chemical Bonding and Aromaticity in Furan, Pyrrole, and Thiophene: A Magnetic Shielding Study. *J. Org. Chem.* **2013**, *78*, 8037–8043. [PubMed]
75. Bruker. *APEX3 and SAINT*; Bruker AXS Inc.: Madison, WI, USA, 2015.
76. Krause, L.; Herbst-Irmer, R.; Sheldrick, G.M.; Stalke, D. Comparison of Silver and Molybdenum Microfocus X-ray Sources for Single-Crystal Structure Determination. *J. Appl. Crystallogr.* **2015**, *48*, 3–10. [CrossRef] [PubMed]
77. Sheldrick, G.M. SHELXT−Integrated Space-Group and Crystal-Structure Determination. *Acta Crystallogr. Sect. A Found. Adv.* **2015**, *71*, 3–8. [CrossRef]
78. Farrugia, L.J. WinGX and ORTEP for Windows: An Update. *J. Appl. Crystallogr.* **2012**, *45*, 849–854. [CrossRef]
79. Grimme, S.; Ehrlich, S.; Goerigk, L. Effect of the damping function in dispersion corrected density functional theory. *J. Comp. Chem.* **2011**, *32*, 1456–1465. [CrossRef]
80. Frisch, M.J.; Trucks, G.W.; Schlegel, H.B.; Scuseria, G.E.; Robb, M.A.; Cheeseman, J.R.; Scalmani, G.; Barone, V.; Mennucci, B.; Petersson, G.A.; et al. *Gaussian 16 Revision B.0.1.*; Gaussian Inc.: Wallingford, CT, USA, 2016.